ELSEVIER

Engineering Analysis with Boundary Elements 32 (2008) 461–470

ENGINEERING ANALYSIS *with* BOUNDARY ELEMENTS

www.elsevier.com/locate/enganabound

New concepts for moving least squares: An interpolating non-singular weighting function and weighted nodal least squares

Thomas Most*, Christian Bucher

Institute of Structural Mechanics Bauhaus, University Weimar, Marienstr. 15, D-99423 Weimar, Germany

Received 28 November 2006; accepted 10 October 2007
Available online 21 February 2008

Abstract

In this paper two new concepts for the classical moving least squares (MLS) approach are presented. The first one is an interpolating weighting function, which leads to MLS shape functions fulfilling the interpolation condition exactly. This enables a direct application of essential boundary conditions in the element-free Galerkin method without additional numerical effort. In contrast to existing approaches using singular weighting functions, this new weighting type leads to regular values of the weights and coefficients matrices in the whole domain even at the support points. The second enhancement is an approach, where the computation of the polynomial coefficient matrices is performed only at the nodes. At the interpolation point then a simple operation leads to the final shape function values. The basis polynomial of each node can be chosen independently which enables the simple realization of a p-adaptive scheme.

Keywords: Moving least squares; Kronecker delta property; Interpolating weighting function; Nodal basis; Weighted polynomials; Element-free Galerkin method

1. Introduction

During the last decade the moving least squares (MLS) method proposed in [1] has become a very popular approximation scheme. We can find a wide range of applications in the framework of function approximation and surface construction [2]. Recently, this method has been applied especially in response surface models in order to accelerate optimization procedures, e.g. in [3], and stochastic analyses, e.g. in [4]. A further important application field are meshless methods, e.g. the diffuse element method (DEM) proposed in [5], the well-known element-free Galerkin (EFG) method introduced in [6] and the meshless local Petrov Galerkin method proposed in [7]. Meshless methods are very common to model problems with moving boundaries such as crack growth in solids, since changing discontinuities can be represented very easily by modifying only the weighting functions which is a well-known advantage compared to the classical finite element method.

Due to the applied local polynomial regression the MLS approach is an approximation method instead of a true interpolation. For several applications, e.g. if noisy data have to be handled, this property is even volitional. For the application in response surface models for structural reliability analyses, this property may cause significant problems. In the framework of a meshless Galerkin scheme the not fulfilled Kronecker delta property of the MLS method requires additional effort for the imposition of the essential boundary conditions. Several methods have been developed to overcome this problem: the use of Lagrange multipliers [6], the use of collocation methods [8,9], the modification of the variational principles [10], the combination with finite elements [11], the application of penalty methods [9], and the use of partition of unity finite element weighting functions presented in [12]. In [13] and [14] special procedures for reproducing kernel methods are presented, where a mixed interpolation based on a normalized kernel function to impose Kronecker delta property and an enrichment function which constitutes reproducing conditions are combined.

*Corresponding author. Tel.: +49 3643 584503; fax: +49 3643 584514.
E-mail address: thomas.most@uni-weimar.de (T. Most).
URL: http://www.uni-weimar.de/~most (T. Most).

0955-7997/$ - see front matter © 2007 Elsevier Ltd. All rights reserved.
doi:10.1016/j.enganabound.2007.10.013

The application of singular weighting functions in the MLS approach, which leads to singular coefficient matrices at the nodes, can impose Kronecker delta property as well, but requires a very careful placement of the integration points. In [15] and [16] special procedures for the handling of such singular matrices were proposed, which require additional numerical effort. In this paper a non-singular weighting function is presented, which leads to an exact fulfillment of the interpolation condition without additional numerical effort. This weighting function leads to regular values of the weights and the coefficient matrices in the whole interpolation domain even at the nodes. Furthermore, this function gives much more stable results for varying size of the influence radius and for strongly distorted nodal arrangements than classical weighting function types.

One of the most time consuming steps in the MLS method is the assembling of the coefficient and weighting matrices and their inversion. This effort increases even more for higher dimensions and higher order base polynomials. Since in the EFG method generally a large number of integration points is used, for which these expensive operations have to be performed, the numerical effort is much higher than in the finite element method. In this paper a new concept is presented, where the least squares coefficients are calculated only at the nodes. At each interpolation point the nodal coefficients are weighted using the improved weighting function. This new method is called weighted nodal least squares (WNLS). Furthermore, this approach enables the independent choice of the polynomial basis for each node, which enables the development of simple p-adaptation schemes.

The advantages of the presented new MLS concepts in comparison to the classical approach are presented by means of several numerical examples.

2. MLS approach

An arbitrary function u is interpolated at a point $\mathbf{x}$ by a polynomial as

$$u^h(\mathbf{x}) = [1 \;\; xy \;\; x^2 \;\; xy \;\; y^2 \;\; \ldots] \begin{bmatrix} a_1 \\ \vdots \\ a_n \end{bmatrix} = \mathbf{p}^{\mathrm{T}}(\mathbf{x})\mathbf{a}, \tag{1}$$

where $\mathbf{p}(\mathbf{x})$ is the base vector and $\mathbf{a}$ contains the coefficients of the polynomial. These coefficients are constant in the interpolation domain and can be determined directly if the number of supporting points m used for the interpolation is equivalent to the number of coefficients n. This principle is applied for example in the finite element method, where an element-wise interpolation is realized. There, the coefficients are simply given as

$$\mathbf{a} = \mathbf{P}^{\mathrm{T}^{-1}}\tilde{\mathbf{u}}, \tag{2}$$

where $\tilde{\mathbf{u}}$ contains the function values at the supporting points

$$\tilde{\mathbf{u}} = [\tilde{u}_1 \;\; \ldots \;\; \tilde{u}_m]^{\mathrm{T}} \tag{3}$$

and $\mathbf{P}$ consists of the values of the polynomial basis calculated at the supporting points

$$\mathbf{P} = \begin{bmatrix} P_1(\mathbf{x}_1) & P_1(\mathbf{x}_2) & \ldots & P_1(\mathbf{x}_m) \\ P_2(\mathbf{x}_1) & P_2(\mathbf{x}_2) & \ldots & P_2(\mathbf{x}_m) \\ \vdots & \vdots & \ddots & \vdots \\ P_n(\mathbf{x}_1) & P_n(\mathbf{x}_2) & \ldots & P_n(\mathbf{x}_m) \end{bmatrix}. \tag{4}$$

Within the MLS approximation method [1] the number of supporting points m exceeds the number of coefficients n, which leads to an overdetermined system of equations. This kind of optimization problem can be solved by using a least squares approach

$$\mathbf{P}\tilde{\mathbf{u}} = \mathbf{P}\mathbf{P}^{\mathrm{T}}\mathbf{a}(\mathbf{x}) \tag{5}$$

with changing ("moving") coefficients $\mathbf{a}(\mathbf{x})$. In order to obtain a local character of the polynomial regression a distance depending weighting function $w = w(s)$ was introduced, where s is the normalized distance between the interpolation point and the considered supporting point

$$s_i = \frac{\|\mathbf{x} - \mathbf{x}_i\|}{D} \tag{6}$$

and D is the influence radius, which is defined as a numerical parameter. All types of functions can be used as weighting function $w(s)$ which have their maximum in $s = 0$ and vanish outside of the influence domain specified by $s = 1$. The nodes whose weighting function values do not vanish at the interpolation point are the influencing nodes of the interpolation point.

Using the introduced weighting function, Eq. (5) is expanded to

$$\mathbf{B}(\mathbf{x})\tilde{\mathbf{u}} = \mathbf{A}(\mathbf{x})\mathbf{a}(\mathbf{x}), \tag{7}$$

where $\mathbf{A}(\mathbf{x})$ and $\mathbf{B}(\mathbf{x})$ are given as

$$\begin{aligned} \mathbf{A}(\mathbf{x}) &= \mathbf{P}\mathbf{W}(\mathbf{x})\mathbf{P}^{\mathrm{T}}, \\ \mathbf{B}(\mathbf{x}) &= \mathbf{P}\mathbf{W}(\mathbf{x}), \end{aligned} \tag{8}$$

and the diagonal matrix $\mathbf{W}(\mathbf{x})$ can be determined as

$$\mathbf{W}(\mathbf{x}) = \begin{bmatrix} w(\mathbf{x} - \mathbf{x}_1) & 0 & \ldots & 0 \\ 0 & w(\mathbf{x} - \mathbf{x}_2) & \ldots & 0 \\ \vdots & \vdots & \ddots & \vdots \\ 0 & 0 & \ldots & w(\mathbf{x} - \mathbf{x}_m) \end{bmatrix}. \tag{9}$$

The interpolated value of the function u at $\mathbf{x}$ can be obtained by introducing the MLS shape functions

$$u^h(\mathbf{x}) = \mathbf{\Phi}^{MLS}(\mathbf{x})\tilde{\mathbf{u}}, \quad \mathbf{\Phi}^{MLS}(\mathbf{x}) = \mathbf{p}^{\mathrm{T}}(\mathbf{x})\mathbf{A}(\mathbf{x})^{-1}\mathbf{B}(\mathbf{x}). \tag{10}$$

Similar to Eq. (2) the invertibility of the matrix $\mathbf{A}(\mathbf{x})$ has to be assured, which is not automatically given if the interpolation point is in the influence domain of at least n nodes.

The MLS approximation does not pass through the nodal values caused by the applied least squares approach.

This implies that the interpolation condition is not fulfilled,

$$\Phi_i^{MLS}(\mathbf{x}_j) \neq \delta_{ij}. \tag{11}$$

3. Weighting functions

A large number of different weighting functions for the MLS approach can be found in the literature. In this section one of the most common weighting types, the Gaussian weighting function, is shortly discussed. This weighting function is of exponential type and can be formulated for infinite support as

$$w_G^{\infty}(s) = \mathrm{e}^{-s^2/\alpha^2}. \tag{12}$$

An infinite support of this weighting function is very practical for data approximation since the resulting function has C^{∞} smoothness. But for an application in the EFG method a compact support is required in order to obtained a sparse stiffness matrix. For this case the weighting function reads

$$w_G(s \leqslant 1) = \frac{\mathrm{e}^{-s^2/\alpha^2} - \mathrm{e}^{-1/\alpha^2}}{1 - \mathrm{e}^{-1/\alpha^2}},$$
$$w_G(s > 1) = 0. \tag{13}$$

In Fig. 1 the Gaussian weighting function is displayed for the one-dimensional case.

Due to the applied least square approach explained in the previous section, the obtained nodal shape functions have a strong dependence on the size of the influence radius D. In Fig. 2 a single nodal shape function of the middle node of a regular one-dimensional set of nodes is shown for increasing D. The figure indicates that with increasing influence radius, the shape function error at each support point, caused by the approximative character of the MLS approach, increases dramatically. This problem is even more significant for irregular nodal setups. As a result the application of geometrical boundary conditions in the EFG method is difficult and additional numerical effort is necessary to fulfill these conditions.

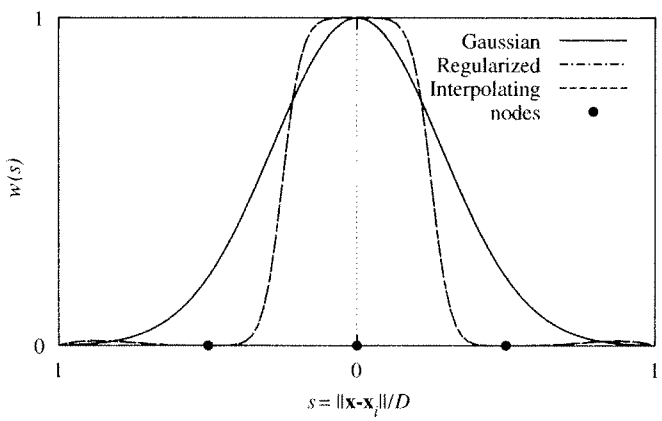

Fig. 1. Gaussian, regularized and new interpolating weighting functions for a single node with neighbor nodes.

Because of the presented problems using classical weighting function types, in [17] the authors presented a regularized weighting function which enables the fulfillment of the MLS interpolation condition with very high accuracy without additional numerical effort

$$\Phi_i^{MLS}(\mathbf{x}_j) \approx \delta_{ij}. \tag{14}$$

The weighting function value of a node i at an interpolation point $\mathbf{x}$ was introduced as follows:

$$w_R(s) = \frac{\tilde{w}_R(s)}{\sum_{j=1}^{m} \tilde{w}_R(s_j)}, \tag{15}$$

with

$$\tilde{w}_R^{\infty}(s) = \varepsilon^2 (s^{\gamma} + \varepsilon)^{-2} \tag{16}$$

for infinite support and with

$$\tilde{w}_R(s \leqslant 1) = \frac{(s^{\gamma} + \varepsilon)^{-2} - (1+\varepsilon)^{-2}}{\varepsilon^{-2} - (1+\varepsilon)^{-2}}, \quad \varepsilon \ll 1,$$
$$\tilde{w}_R(s > 1) = 0 \tag{17}$$

for compact support. In [17] it is recommended to choose the regularization parameter ε as

$$\varepsilon = 10^{-5} \tag{18}$$

and the exponent is taken as $\gamma = 2$. In Fig. 1 the regularized weighting function is displayed additionally as a function of the standardized distance s and the position of the supporting points. In Fig. 2 a single nodal shape function obtained by using the regularized weighting function type is shown for different values of the influence radius D. The figure clearly points out that the interpolation condition is fulfilled with very high accuracy even for irregular sets of nodes with grading node density. In clear contrast to the shape functions obtained with the Gaussian weighting function the influence radius D influences the regularized shape function characteristics marginally if a certain value of D is reached.

In this paper the regularized weighting type is enhanced in order to obtain a true interpolation MLS approach. Based on the following formulation for compact support:

$$w_I(s) = \frac{s^{-\alpha} - 1}{\sum_{j=1}^{m} (s_j^{-\alpha} - 1)}, \tag{19}$$

which cannot be evaluated numerically at the support points, the following final weighting function is formulated:

$$w_I(s) = \frac{s_i^{\alpha}(s^{-\alpha} - 1)}{s_i^{\alpha} \sum_{j=1}^{m} (s_j^{-\alpha} - 1)}, \tag{20}$$

where s_i denotes the distance to the closest support point. Eq. (20) can be simplified as

$$w_I(s_i \leqslant 1) = \frac{1 - s_i^{\alpha}}{1 + s_i^{\alpha} \sum_{j=1, j\neq i}^{m} s_j^{-\alpha} + s_i^{\alpha} m},$$
$$w_I(s_{j\neq i} \leqslant 1) = \frac{s_i^{\alpha}(s_j^{-\alpha} - 1)}{1 + s_i^{\alpha} \sum_{j=1, j\neq i}^{m} s_j^{-\alpha} + s_i^{\alpha} m},$$
$$w_I(s > 1) = 0. \tag{21}$$

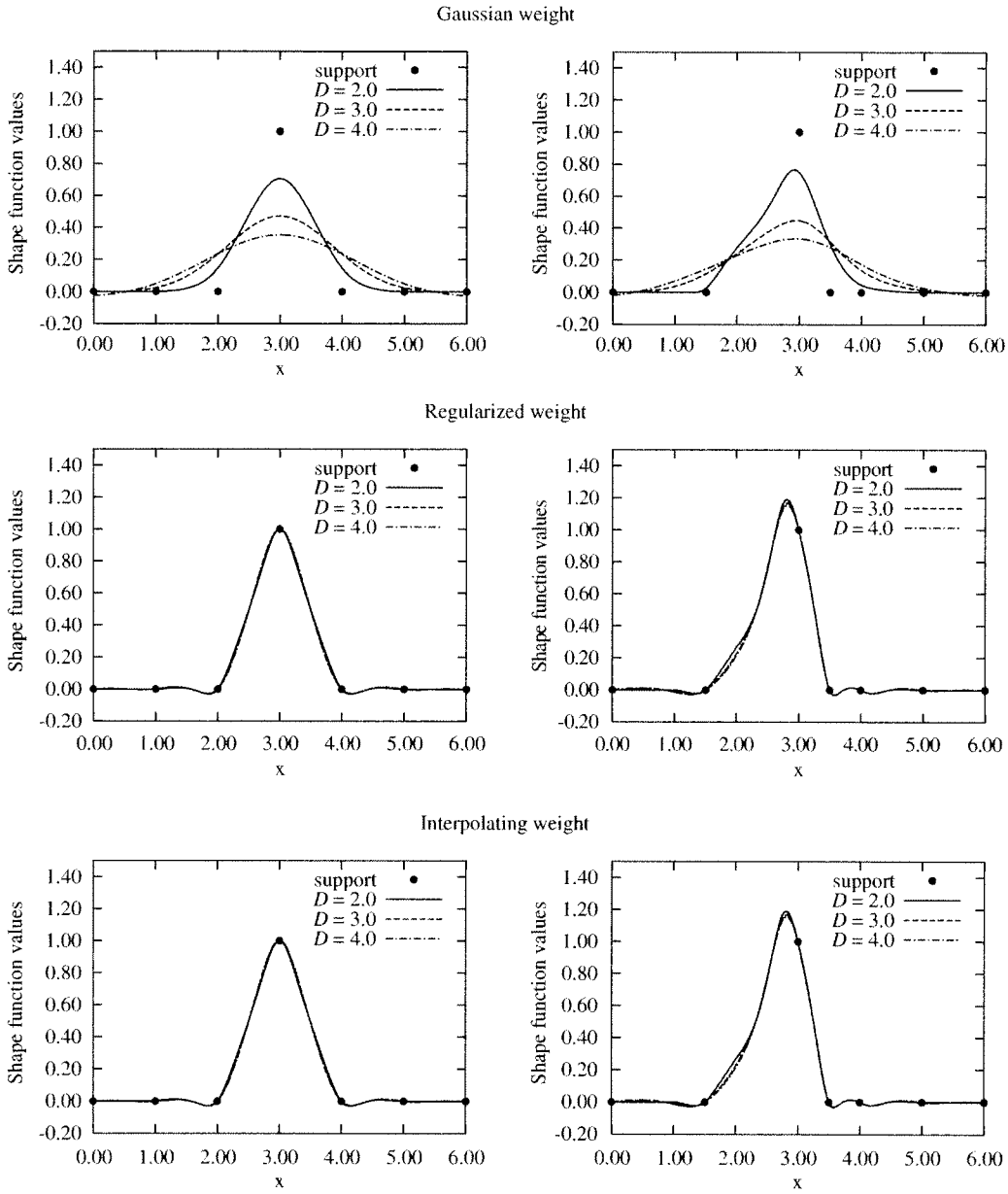

Fig. 2. Nodal shape function of the MLS interpolation with Gaussian, regularized and interpolating weighting function and linear polynomial basis for regular and irregular sets of nodes.

For infinite support we obtain analogously

$$w_I^{\infty}(s_i) = \frac{1}{1 + s_i^{\alpha}\sum_{j=1,j\neq i}^{m} s_j^{-\alpha}},$$
$$w_I^{\infty}(s_{j\neq i}) = \frac{s_i^{\alpha} s_j^{-\alpha}}{1 + s_i^{\alpha}\sum_{j=1,j\neq i}^{m} s_j^{-\alpha}}. \tag{22}$$

If no pair of support points with equal positions exists, the weighting function in Eq. (21) provides always regular numerical values even at all support points, where we obtain

$$w_I(s_i = 0) = \frac{1 - s_i^{\alpha}}{1 + s_i^{\alpha}\sum_{j=1,j\neq i}^{m} s_j^{-\alpha} + s_i^{\alpha} m} = \frac{1 - 0}{1 + 0 \cdot \sum_{j=1,j\neq i}^{m} s_j^{-\alpha} + 0 \cdot m} = 1,$$

$$w_I(s_{j\neq i}) = \frac{s_i^{\alpha}(s_j^{-\alpha} - 1)}{1 + s_i^{\alpha}\sum_{j=1,j\neq i}^{m} s_j^{-\alpha} + s_i^{\alpha} m} = \frac{0 \cdot (s_j^{-\alpha} - 1)}{1 + 0 \cdot \sum_{j=1,j\neq i}^{m} s_j^{-\alpha} + 0 \cdot m} = 0. \tag{23}$$

In this paper the exponent is chosen as $\alpha = 4$. In Figs. 1 and 2 the shape functions using this interpolating weighting type are displayed, which show no visible deviation to the shape functions obtained with the almost interpolating regularized weighting type.

For two-dimensional (2D) and three dimensional (3D) problems the essential boundary conditions are fulfilled only at the nodes through the non-zero intercepts of internal nodes with the domain boundary. In [18] a concept

for the blending of internal weighting functions was presented, which could solve this problem. For the sake of simplicity this approach is not used in this paper, which means that the essential boundary conditions are fulfilled only point-wisely. For pure data interpolation problems this fact does not play any role.

4. Weighted nodal least squares

One of the most time consuming steps in the MLS approach is the assembling of the coefficient and weighting matrices and the inversion of the matrix $\mathbf{A}(\mathbf{x})$ in Eq. (10). This effort increases even more for higher dimensions and higher order base polynomials.

Since in the EFG method generally a large number of integration points are used, where these expensive operations have to be performed, the numerical effort is much higher than in the finite element method. In this paper a new concept is presented, where the least squares coefficients are calculated only at the nodes

$$\mathbf{a}(\mathbf{x}_I) = \mathbf{A}(\mathbf{x}_I)^{-1}\mathbf{B}(\mathbf{x}_I)\tilde{\mathbf{u}}. \tag{24}$$

At each interpolation point the nodal coefficients are weighted using the new weighting function. The final interpolation reads

$$u^h(\mathbf{x}) = \frac{\sum_{I=1}^{m} w_I(\mathbf{x})\mathbf{p}_I^{\mathrm{T}}(\mathbf{x})\mathbf{a}(\mathbf{x}_I)}{\sum_{I=1}^{m} w_I(\mathbf{x})}. \tag{25}$$

This leads to the WNLS shape functions

$$\mathbf{\Phi}^{WNLS}(\mathbf{x}) = \frac{\sum_{I=1}^{m} w_I(\mathbf{x})\mathbf{p}_I^{\mathrm{T}}(\mathbf{x})\mathbf{Q}(\mathbf{x}_I)}{\sum_{I=1}^{m} w_I(\mathbf{x})} \tag{26}$$

with

$$\mathbf{Q}(\mathbf{x}_I) = \mathbf{A}(\mathbf{x}_I)^{-1}\mathbf{B}(\mathbf{x}_I). \tag{27}$$

The coefficient matrix $\mathbf{Q}(\mathbf{x}_I)$ has to be calculated only for the nodes, which is much less time consuming than the inversion of $\mathbf{A}(\mathbf{x})$ for each interpolation point, since the number of nodes is generally much smaller than the number of integration points. Another benefit of this method is shown in Eq. (25), where $\mathbf{p}_I^{\mathrm{T}}(\mathbf{x})$ is the polynomial basis, which can be chosen independently for every node in contrast to the standard MLS approach. This enables a very easy p-adaptivity scheme.

The presented WNLS methods has some similar aspects as the method of finite spheres (MFS) proposed in [19]. In the MFS a Shepard method is used to interpolate the coefficients of an extrinsic basis. In WNLS the coefficients of the intrinsic basis are computed at each node by the MLS approach and the obtained coefficients are interpolated similarly by a Shepard approach. This means that in the MFS the number of degrees of freedom at each node depends on the basis whereby in the WNLS method only the displacements are the degrees of freedom independently of the basis function. On the other hand the size of the nodal influence domains has to be increased in the WNLS method for higher order basis functions, whereby in the MFS the nodal influence domains can be used unchanged.

The derivative of the WNLS shape functions reads

$$\Phi_{,i}^{WNLS} = \left[\sum_{I=1}^{m}(w_{I,i}(\mathbf{x})\mathbf{p}_I^{\mathrm{T}}(\mathbf{x}) + w_I(\mathbf{x})\mathbf{p}_{I,i}^{\mathrm{T}}(\mathbf{x}))\mathbf{Q}(\mathbf{x}_I)\sum_{I=1}^{m} w_I(\mathbf{x}) - \sum_{I=1}^{m} w_I(\mathbf{x})\mathbf{p}_I^{\mathrm{T}}(\mathbf{x})\mathbf{Q}(\mathbf{x}_I)\sum_{I=1}^{m} w_{I,i}(\mathbf{x})\right]\left[\sum_{I=1}^{m} w_I(\mathbf{x})\right]^{-2}. \tag{28}$$

The computation of the coefficient matrix $\mathbf{Q}(\mathbf{x}_I)$ is required only in the Galerkin method, where the shape functions and their derivatives are used to compute the system vectors and matrices. For data interpolation purposes the coefficients $\mathbf{a}(\mathbf{x}_I)$ at the data points can be calculated directly from the given function values and only their values have to be stored for each data point. The interpolation by using Eq. (25) is then straightforward.

The interpolating weighting function which was presented above cannot be applied in the WNLS approach, since the inversion of the $\mathbf{A}(\mathbf{x})$ at the nodal positions is not possible due to the weighting function values equal to zero. Thus, in the WNLS approach, the regularized weighting type with $\gamma = 1$ is applied in this paper. In Fig. 3 one-dimensional WNLS shape functions are shown depending on the influence radius for this regularized weighting type.

5. Numerical examples

5.1. MLS-shape functions for regular and irregular sets of nodes

Within this example the interpolation errors are calculated for a regular and an irregular set of 5×5 nodes with a distance of $a = 0.25\,\mathrm{m}$ by using the Gaussian, the regularized, and the interpolating weighting functions. In Fig. 4 both investigated nodal sets are displayed.

First the interpolation error at the supporting points for the shape function of node A is analyzed for a varying influence radius D using the regular nodal set. The regularization term for the regularized weighting function is assumed to be $\varepsilon = 10^{-5}$ and the Gaussian shape parameter is taken with $\alpha = 0.3295$.

In Table 1 the obtained maximum error is given for all investigated weighting types. It can be seen that with increasing influence radius the error using the Gaussian weighting function increases but the error from the regularized type remains very small. Furthermore, the interpolating weighting type leads to exact fulfillment of the interpolation condition.

The influence of the minimum nodal distance on the interpolation accuracy is investigated on the irregular set of nodes shown in Fig. 4 by decreasing the distance between nodes A and B. The influence radius is kept constant with $D = 0.5\,\mathrm{m}$. In Table 2 the obtained interpolation errors are given.

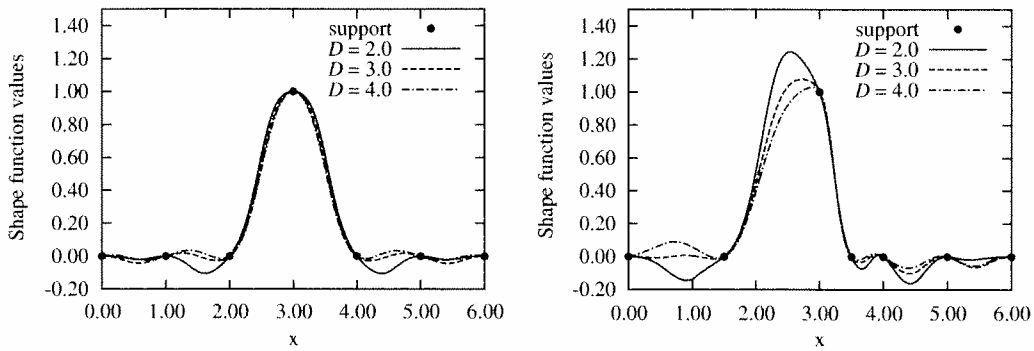

Fig. 3. WNLS shape functions with regularized weighting function and linear basis.

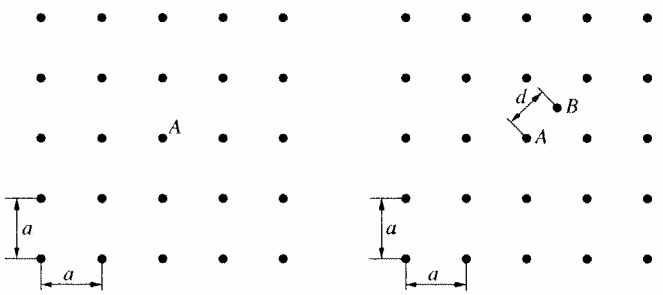

Fig. 4. Investigated regular and irregular sets of nodes.

Table 1
Maximum interpolation error at the nodes as a function of the influence radius using Gaussian (G), regularized (R) and interpolating (I) weighting types

D (m)	$\lvert\Phi_{i,G}^{MLS}(\mathbf{x}_j) - \delta_{ij}\rvert_{max}$ (%)	$\lvert\Phi_{i,R}^{MLS}(\mathbf{x}_j) - \delta_{ij}\rvert_{max}$ (%)	$\lvert\Phi_{i,I}^{MLS}(\mathbf{x}_j) - \delta_{ij}\rvert_{max}$
0.3	0.6	4.29×10^{-8}	0
0.4	10.1	2.48×10^{-7}	0
0.5	30.5	7.20×10^{-7}	0
0.6	49.5	1.65×10^{-6}	0
1.0	81.5	1.42×10^{-5}	0

Table 2
Maximum numerical error as a function of the minimum nodal distance

d_{AB}/D	$\lvert\Phi_{i,G}^{MLS}(\mathbf{x}_j) - \delta_{ij}\rvert_{max}$ (%)	$\lvert\Phi_{i,R}^{MLS}(\mathbf{x}_j) - \delta_{ij}\rvert_{max}$ (%)	$\lvert\Phi_{i,I}^{MLS}(\mathbf{x}_j) - \delta_{ij}\rvert_{max}$
0.4	36.8	9.61×10^{-7}	0
0.2	47.7	2.57×10^{-6}	0
0.1	55.2	1.02×10^{-5}	0
0.01	59.0	1.05×10^{-3}	0
0.001	59.0	1.05×10^{-1}	0

The table clearly indicates that the interpolation error by using the regularized weighting function is very small for larger values of d_{AB}/D and increases for decreasing minimum nodal distance. The application of the interpolating weighting function leads again to an exactly fulfilled interpolation condition.

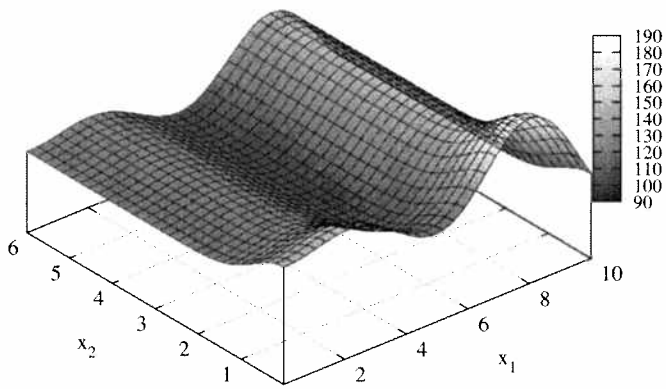

Fig. 5. Investigated nonlinear two-dimensional function.

5.2. Approximation of a nonlinear function

In this example, the approximation quality of the MLS and the WNLS approaches is investigated by means of the two-dimensional nonlinear function

$$f(x_1, x_2) = (30 + x_1 \sin(x_1))(4 + \exp(-x_2^2)). \tag{29}$$

According to [20] the function in Eq. (29) is investigated in the interval

$$0 \leqslant x_1 \leqslant 10, \quad 0 \leqslant x_2 \leqslant 6 \tag{30}$$

by using 7×7 regular distributed support points. In Fig. 5 the investigated function is shown.

In the numerical analyses the MLS approach with exponential and interpolating weighting function and the WNLS method with regularized weighting are used with infinite support of the weighting functions. The approximation error is calculated using the normalized root mean squared error (NRMSE) according to [20] which is defined as

$$\eta_{NRMSE} = \sqrt{\frac{\sum_{k=1}^{K}(f(x_1^k, x_2^k) - \tilde{f}(x_1^k, x_2^k))^2}{\sum_{k=1}^{K}(f(x_1^k, x_2^k))^2}}, \tag{31}$$

where $\tilde{f}(x_1, x_2)$ is the approximated function value and K is the set of evaluation points, which is taken here with 100×100 regular distributed points.

In Fig. 6 the calculated approximation errors are shown depending on the influence radius D of the weighting functions.

The figure indicates that the approximation error increases with increasing influence radius if the exponential weighting type is used. For the application of the interpolating MLS approach and the WNLS method with regularized weight the calculated errors are similar and almost independent of the influence radius.

Finally, the required numerical effort is compared for the presented methods. In Table 3 the computational time needed for 7×7 support points on a standard PC (Intel P4 3.4 GHz) is given for different numbers of evaluation points. The results point out that the interpolating and regularized weighting require similar numerical effort in the MLS and WNLS methods as the exponential weighting. The application of the WNLS approach reduces the numerical effort significantly compared to the MLS method.

5.3. Cantilever with increasing distortion

Within this example the accuracy of the meshless interpolation embedded in a Galerkin method is investigated for a quadratic displacement field as a function of increasing distortion of the nodal arrangement. In Fig. 7 the system with geometrical properties and boundary conditions is shown. For comparison the investigated beam was discretized with four-node (Q4) and nine-node (Q9) iso-parametric finite elements. In Fig. 7 the Q9 discretization is shown exemplarily. The material was assumed to be linear elastic and the properties are taken as $3000\,\mathrm{N/m^2}$ for the Young's modulus and $\nu = 0.0$ for the Poisson's ratio and the thickness was defined to be 0.1 m.

In Fig. 8 the obtained maximum nodal displacement errors using the MLS interpolation with the common Gaussian weighting and the interpolating weighting and using the WNLS approach are displayed as a function of increasing distortion a. The integration is done using Gauss quadrature over 25 integration points per triangular cell and a bilinear base polynomial is taken with an influence radius $D = 2.5\,\mathrm{m}$.

By using the Q9 finite elements the analytical solution was obtained within the machine precision for every distorted system. With increasing distortion the usage of the Gaussian weighting function results in an increasing error, whereby the application of the regularized types

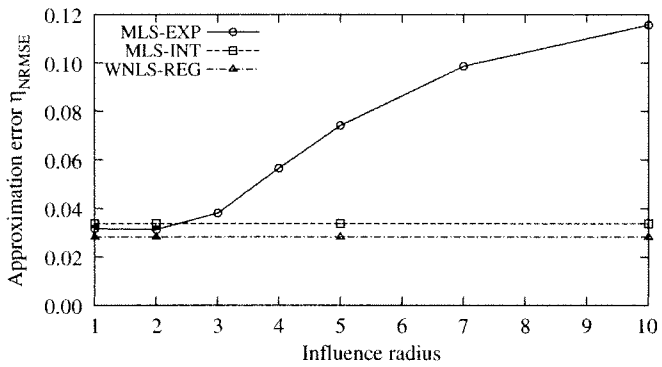

Fig. 6. Approximation errors depending on the influence radius.

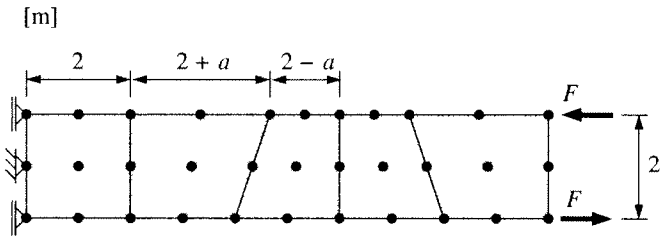

Fig. 7. Investigated distorted cantilever with Q9 mesh.

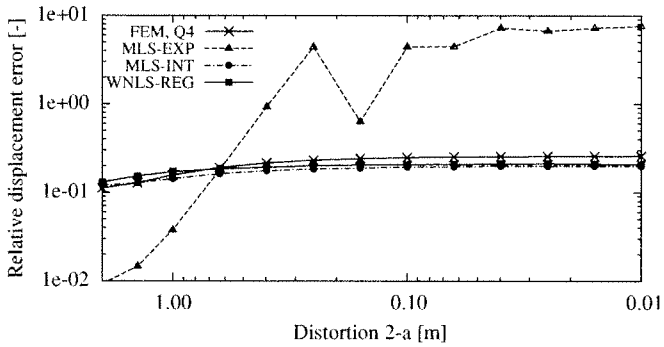

Fig. 8. Maximum nodal errors under increasing distortion obtained by using MLS and WNLS interpolation with Gaussian, regularized and interpolating weighting types.

Table 3
Required computational time in seconds for the function approximation depending on the number of evaluation points

Number of evaluation points		20 × 20	50 × 50	100 × 100	200 × 200	500 × 500
MLS-INT	Linear base	0.00	0.03	0.13	0.54	3.41
WNLS-REG	Linear base	0.00	0.03	0.05	0.19	0.26
MLS-INT	Quadratic base	0.01	0.06	0.29	1.01	6.31
WNLS-REG	Quadratic base	0.01	0.02	0.06	0.21	1.53
MLS-EXP	Linear base	0.01	0.04	0.15	0.60	3.61
WNLS-EXP	Linear base	0.01	0.02	0.05	0.24	1.44
MLS-EXP	Quadratic base	0.01	0.06	0.26	1.04	6.41
WNLS-EXP	Quadratic base	0.01	0.02	0.06	0.26	1.57

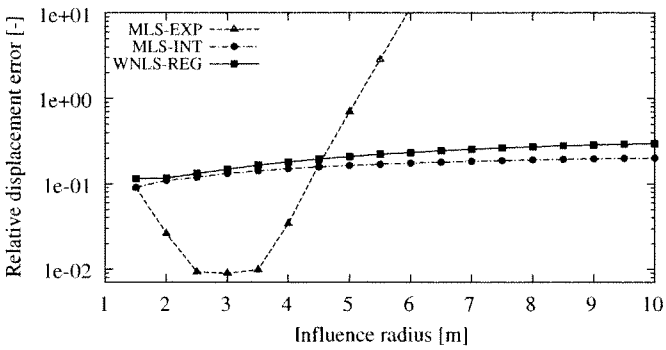

Fig. 9. Maximum nodal error depending on the influence radius D.

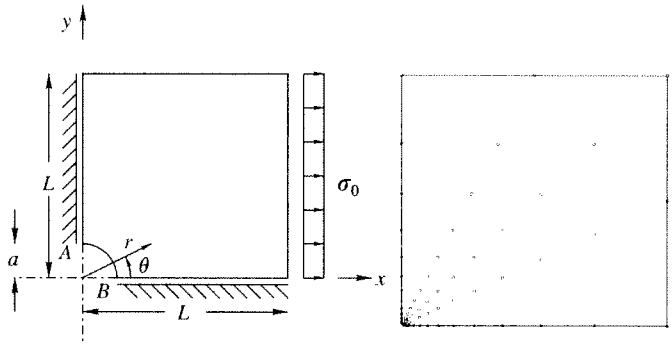

Fig. 10. Infinite plate with a hole and investigated meshless discretization with 65 nodes.

gives very good results even for stronger distortions. The results from the regularized weighting function type are slightly better than those obtained with the Q4 finite elements. The errors obtained with the WNLS approach are similar as those of the MLS interpolation.

Furthermore, the influence of the size of the influence radius D on the displacement errors is investigated for the MLS and WNLS interpolation. In Fig. 9 the obtained errors using the Gaussian, the regularized and the interpolating weighting functions are shown for an undistorted structure depending on the influence radius D. The figure indicates that the results obtained with the regularized and interpolating weighting types are almost independent of the influence radius size in strong contrast to those from the Gaussian weighting function.

5.4. Plate with a hole

In this example an infinite plate with a hole is investigated under tension loading. This benchmark was proposed in [21]. In Fig. 10 the system with loading and boundary conditions is shown. Due to the symmetry of the plate, in the numerical analysis only one quarter is discretized. In order to approximate an infinite plate the ratio between the hole radius a and the half plate length L is taken very small as $a/L = 0.01$. The analytical solution is given in [21] as

$$u_x(r,\theta) = \frac{a}{8G}\left(\frac{r}{a}(\kappa+1)\cos(\theta) + 2\frac{a}{r}[(1+\kappa)\cos(\theta) + \cos(3\theta)] - 2\frac{a^3}{r^3}\cos(3\theta)\right),$$

$$u_y(r,\theta) = \frac{a}{8G}\left(\frac{r}{a}(\kappa-3)\sin(\theta) + 2\frac{a}{r}[(1-\kappa)\sin(\theta) + \sin(3\theta)] - 2\frac{a^3}{r^3}\sin(3\theta)\right), \quad (32)$$

for the displacement, and

$$\sigma_{xx}(r,\theta) = 1 - \frac{a^2}{r^2}\left(\frac{3}{2}\cos(2\theta) + \cos(4\theta)\right) + \frac{3}{2}\frac{a^4}{r^4}\cos(4\theta),$$

$$\sigma_{xy}(r,\theta) = -\frac{a^2}{r^2}\left(\frac{1}{2}\sin(2\theta) + \sin(4\theta)\right) + \frac{3}{2}\frac{a^4}{r^4}\sin(4\theta),$$

$$\sigma_{yy}(r,\theta) = -\frac{a^2}{r^2}\left(\frac{1}{2}\cos(2\theta) - \cos(4\theta)\right) - \frac{3}{2}\frac{a^4}{r^4}\cos(4\theta) \quad (33)$$

for the stresses, where G is the shear modulus and κ indicates the Kolosov constant. For plane stress conditions $\kappa = (3-\nu)/(1+\nu)$.

The numerical analyses are carried out by investigating three different discretization levels with 65, 341 and 2133 nodes with different basis polynomials. Fig. 10 shows the discretization with 65 nodes. The figure indicates that the node density increases with decreasing distance to the hole. This is similar for all three discretizations. As in the previous example 25 Gauss integration points are used per triangular integration cell. Due to the varying node density the influence radius is chosen for each node individually according to [22] as

$$D_I = \beta \cdot r_{I_{max}}, \quad \beta > 1, \quad (34)$$

with

$$r_{I_{max}} = \max\|\mathbf{x}_i - \mathbf{x}_I\|, \quad i \in J_I^N, \quad (35)$$

where J_I^N represents the set of natural neighbor nodes of node I. Natural neighbor nodes of I are those nodes, which share a common edge with I in the Voronoi diagram [23].

As error measure the relative energy error is used which is defined as

$$\eta_E = \frac{\|\mathbf{u}^h - \mathbf{u}\|_E}{\|\mathbf{u}\|_E} = \frac{\sqrt{\frac{1}{2}\int_\Omega (\boldsymbol{\varepsilon}^h - \boldsymbol{\varepsilon})^{\mathrm{T}}\mathbf{C}(\boldsymbol{\varepsilon}^h - \boldsymbol{\varepsilon})}}{\sqrt{\frac{1}{2}\int_\Omega \boldsymbol{\varepsilon}^{\mathrm{T}}\mathbf{C}\boldsymbol{\varepsilon}}}. \quad (36)$$

In Fig. 11 the obtained errors are shown for the MLS and WNLS approaches with a linear and quadratic basis for all nodes. The scaling factor β in Eq. (34) is taken as $\beta = 1.3$ for the linear basis and $\beta = 2.5$ for the quadratic basis. The figure indicates a very good agreement of the MLS and WNLS results with almost theoretical convergency rates.

Finally, the WNLS method with combined linear and quadratic nodal basis is applied. For this purpose the nodes with a given distance to the hole center are taken with

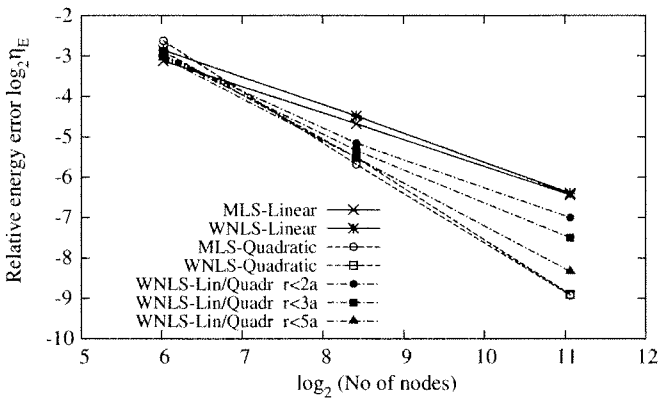

Fig. 11. Relative energy error η_E for the plate with a hole problem depending on the discretization for MLS and WNLS with uniform nodal base polynomials and WNLS with combined linear and quadratic nodal base.

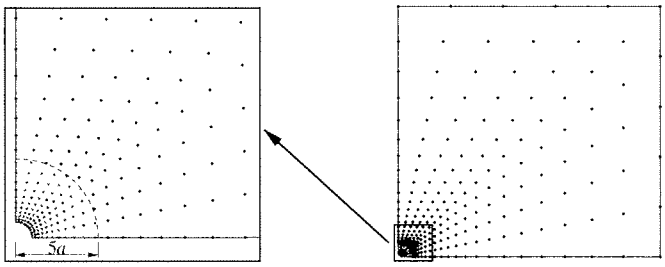

Fig. 12. Nodes with quadratic base (blue dots) around the hole with $r \leqslant 5a$ and linear base (black diamonds) in the remaining domain.

quadratic basis and the remaining nodes with linear basis. Fig. 12 shows the nodes with quadratic and linear basis.

Three different cases are investigated with $r \leqslant 2a$, $r \leqslant 3a$ and $r \leqslant 5a$. The results are shown in Fig. 11. As indicated in the figure the relative error decreases by using the combined linear and quadratic basis compared to the pure linear basis. If the nodes with $r \leqslant 5a$ are taken with the quadratic basis the convergency rate is very close to this of the full quadratic setup, while two third of all nodes still use the linear base.

6. Conclusion

In this paper two new concepts for the classical moving least squares (MLS) approach have been presented. The first one is a non-singular interpolating weighting function, which leads to MLS shape functions fulfilling the interpolation condition exactly. This enables a direct application of essential boundary conditions without additional numerical effort. Furthermore, this weighting function leads to results, which are much more independent of a distortion of the nodal configuration and the size of the influence domain as these obtained with classical weighting types. Nevertheless, for practical applications the results are similar as those obtained with the regularized weighting type presented by the authors in previous publications.

The second enhancement is the so-called weighted nodal least squares (WNLS) approach, where the computation of the polynomial coefficient matrices is performed only at the nodes. At the interpolation point than a simple operation leads to the final shape function values. For function interpolation purposes this approach is significantly more efficient than the classical MLS method by obtaining a similar accuracy. The basis polynomial of each node can be chosen independently which enables the realization of a simple p-adaptive scheme. This can reduce the numerical effort in an Galerkin scheme for several problems, where high order approximations are necessary in local regions but the global trend can be represented by a low order approximation. However, the efficiency of the application in a Galerkin method can be low since the bandwidth of the interpolation is increased compared to classical MLS and consequently the calculation of the stiffness matrix needs more operations. An application for global solution schemes without the need of the stiffness matrix would be more promising.

Acknowledgment

This research has been supported by the German Research Council (DFG) under Grant no. BU 987/9-1, which is gratefully acknowledged by the authors.

References

[1] Lancaster P, Salkauskas K. Surface generated by moving least squares methods. Math Comput 1981;37:141–58.
[2] Levin D. The approximation power of moving least-squares. Math Comput 1998;67(224):1517–31.
[3] Breitkopf P, Naceur H, Rassineux A, Villon P. Moving least squares response surface approximation: formulation and metal forming applications. Comput Struct 2005;83:1411–28.
[4] Bucher C, Macke M, Most T. Approximate response functions in structural reliability analysis. In: Spanos P, Deodatis G, editors. Proceedings of the fifth computational stochastic mechanics conference, Rhodos, Greece, June 21–23, 2006. Balkema; 2006.
[5] Nayroles B, Touzot G, Villon P. Generalizing the FEM: diffuse approximations and diffuse elements. Comput Mech 1992;10:307–18.
[6] Belytschko T, Lu YY, Gu L. Element-free Galerkin methods. Int J Numer Methods Eng 1994;37:229–56.
[7] Atluri SN, Zhu T. A new meshless local Petrov–Galerkin (MLPG) approach in computational mechanics. Comput Mech 1998;22: 117–27.
[8] Belytschko T, Tabbara M. Dynamic fracture using element-free Galerkin method. Int J Numer Methods Eng 1996;39:141–58.
[9] Zhu T, Atluri N. Modified collocation method and a penalty function for enforcing essential boundary conditions in the element-free Galerkin method. Comput Mech 1998;21:211–22.
[10] Lu YY, Belytschko T, Gu L. A new implementation of the element-free Galerkin method. Comput Methods Appl Mech Eng 1994;113: 397–414.
[11] Krongauz Y, Belytschko T. Enforcement of essential boundary conditions in meshless approximations using finite elements. Comput Methods Appl Mech Eng 1996;131:133–45.
[12] Alves MK, Rossi R. A modified element-free Galerkin method with essential boundary conditions enforced by an extended partition of unity finite element weight function. Int J Numer Methods Eng 2003; 57:1523–52.

[13] Chen JS, Wang HP. New boundary condition treatments in meshless computation of contact problems. Comput Methods Appl Mech Eng 2000;187:441–68.
[14] Chen JS, Han W, You Y, Meng X. A reproducing kernel method with nodal interpolation property. Int J Numer Methods Eng 2003; 56:935–60.
[15] Kaljevic I, Saigal S. An improved element free Galerkin formulation. Int J Numer Methods Eng 1997;40:2953–74.
[16] Kunle M. Entwicklung und Untersuchung von Moving Least Square Verfahren zur numerischen Simulation hydrodynamischer Gleichungen. PhD thesis, Eberhard-Karls-University Tübingen, Germany; 2001.
[17] Most T, Bucher C. A moving least squares weighting function for the element-free Galerkin method which almost fulfills essential boundary conditions. Struct Eng Mech 2005;21(3):315–32.
[18] Most T. Stochastic crack growth simulation in reinforced concrete structures by means of coupled finite element and meshless methods. PhD thesis, Bauhaus University Weimar, Germany; 2005.
[19] De S, Bathe KJ. The method of finite spheres. Comput Mech 2000; 25:329–45.
[20] Mullur AA. A new response surface paradigm for computationally efficient multiobjective optimization. PhD thesis, Rensselear Polytechnic Institute, Troy, New York; 2005.
[21] Timoshenko SP, Goodier JN. Theory of elasticity. 3rd ed. New York: McGraw Hill; 1970.
[22] Most T. A natural neighbor based moving least squares approach for the element-free Galerkin method. Int J Numer Methods Eng 2007; 71(2):224–52.
[23] Green PJ, Sibson RR. Computing dirichlet tessellations in the plane. Comput J 1978;21:168–73.